



**HAL**  
open science

## A method to assess the suffusion susceptibility of low permeability core soils in compacted dams based on construction data

Lingran Zhang, Rachel Gelet, Didier Marot, Marc Smith, Jean-Marie Konrad

### ► To cite this version:

Lingran Zhang, Rachel Gelet, Didier Marot, Marc Smith, Jean-Marie Konrad. A method to assess the suffusion susceptibility of low permeability core soils in compacted dams based on construction data. *European Journal of Environmental and Civil Engineering*, 2018, 23 (5), pp.626-644. 10.1080/19648189.2018.1474386 . hal-04168000

**HAL Id: hal-04168000**

**<https://hal.science/hal-04168000>**

Submitted on 21 Jul 2023

**HAL** is a multi-disciplinary open access archive for the deposit and dissemination of scientific research documents, whether they are published or not. The documents may come from teaching and research institutions in France or abroad, or from public or private research centers.

L'archive ouverte pluridisciplinaire **HAL**, est destinée au dépôt et à la diffusion de documents scientifiques de niveau recherche, publiés ou non, émanant des établissements d'enseignement et de recherche français ou étrangers, des laboratoires publics ou privés.

# **A method to assess the suffusion susceptibility of low permeability core soils in compacted dams based on construction data**

Lingran Zhang<sup>a</sup>, Rachel Gelet <sup>a\*</sup>, Didier Marot<sup>a</sup>, Marc Smith<sup>b</sup> and Jean-Marie Konrad<sup>c</sup>

*<sup>a</sup> Institut de Recherche en Génie Civil et Mécanique, Université de Nantes / CNRS, IUT de Saint-Nazaire, 58 rue Michel Ange, F-44606 Saint-Nazaire, France*

*<sup>b</sup> Hydro Québec, 75 René-Lévesque West, 3<sup>rd</sup> floor, Montréal, QC H2Z 1A4, Canada*

*<sup>c</sup> Laval University, Civil Engineering Department, Adrien-Pouliot Pavilion, Québec, QC G1K 7P4, Canada*

*\*corresponding author: rachel.gelet@univ-nantes.fr*

## **A method to assess the suffusion susceptibility of core soils in compacted dams based on construction data**

Suffusion, as one of the main internal erosion processes in earth structures and their foundations, may increase their failure risks. The paper aims at presenting a general method to assess the suffusion susceptibility of core soil samples belonging to zoned hydraulic embankment dams. On one hand, the suffusion susceptibility of the soil samples is evaluated by an erosion resistance index. Thanks to existing statistical analyses, the erosion resistance index is estimated from several soil parameters that can be easily measured in-situ or in laboratory during the construction of a dam. On the other hand, the saturated hydraulic conductivity of the soil samples is evaluated based on the amount of fines content and on available construction data. Moreover, the power dissipated by the flow is inferred based on the saturated hydraulic conductivity and simplified fluid boundary conditions. The combined consideration of the erosion resistant index and of the power dissipated by the flow permits to identify zones characterized with a relatively larger suffusion potential (lower erosion resistance index and larger power than their respective average). Throughout, the method is applied to a particular zoned dam with a till core, from Northern Quebec, as a proof of concept.

Keywords: embankment dam; internal erosion; erosion resistance index; suffusion susceptibility; energy approach

## **1. Introduction**

Internal erosion is one of the main causes of embankment dam failures (Foster et al., 2000). Based on the physics of the process and on its location within a structure, four types of internal erosion can be identified: concentrated leak erosion, backward erosion, contact erosion and suffusion (Fry, 2012). Suffusion is a complex process that under seepage flow, the fine solid particles can be detached, transported, and for some of them blocked. The finer fraction eroded and leaving the coarse matrix of the soil may further modify the hydraulic conductivity and the mechanical parameters of the soil. On-going suffusion may result in an increase of permeability, greater seepage velocities, and potentially higher hydraulic gradients, possibly accelerating the rate of suffusion (ICOLD, 2013). The development of suffusion gives rise to a wide range of dam incidents including piping and sinkholes.

Several researches in the literature assume that suffusion is best represented by its initiation. The main initiation conditions for suffusion comprise three components: material susceptibility, critical hydraulic load, and critical stress condition (Garner et al., 2010). Several methods have been proposed to characterize the initiation of suffusion confronting material susceptibility criteria and hydraulic criteria (Marot and Benamar, 2012). With the objective to evaluate the likelihood of suffusion initiation, several criteria based on the study of grain size distribution have been proposed in literature (Kenney and Lau, 1985; Li and Fannin, 2008, among others). Wan and Fell (2008) concluded that the most widely used methods based on particle size distribution are conservative. Kovacs (1981) recognized that even if the geometrical conditions allow particle movements, the hydraulic conditions have to be studied. Three approaches have been proposed to describe the hydraulic action on particles: the hydraulic gradient (Skempton and Brogan, 1994; Li, 2008), the hydraulic shear stress (Reddi et al., 2000) and the pore velocity

(Perzmaier et al., 2007). However, suffusion tests carried out with permeameters of different sizes indicate that scale effects exist when measuring critical hydraulic criteria (Li, 2008; Marot et al., 2012a). Particularly, Marot et al., (2012a) pointed out that the critical hydraulic gradient concept depends on the length of the seepage path. Moreover, Rochim et al. (2017) showed the significant effect of hydraulic loading history on the value of the critical hydraulic gradient. In the same manner, the authors demonstrated that the critical hydraulic load based on the rate of erosion is influenced by the hydraulic loading history. Therefore these approaches cannot be generalized nor be used directly to evaluate the suffusion susceptibility at dam scales.

Alternatively, Marot et al. (2011) focused on the improvement of the material susceptibility estimation. This estimation is not based on the sole initiation, rather the whole suffusion process is considered. The authors proposed an energy approach to evaluate the material susceptibility of soils based on suffusion experiments performed up to a "final state". This "final state" is obtained towards the end of each test when the hydraulic conductivity is constant while the rate of erosion decreases. This final state is interpreted as being the end of the suffusion process (Le et al., 2017). The hydraulic loading is characterized by the cumulative energy dissipated by the water seepage  $E_{flow}$ . The response of the sample is related to the standard measure of the total dry eroded mass during the whole test  $m_{eroded}$ , and the erosion resistance index is expressed by:

$$I_{\alpha} = - \text{Log} \left( \frac{m_{eroded}}{E_{flow}} \right) \quad (1)$$

Based on this index, a gradual classification is proposed from highly resistant to highly erodible (Marot et al., 2016). Since the erosion resistance index  $I_{\alpha}$  has been proven to be intrinsic, i.e. independent of the sample size (Zhong et al., 2017) and of the loading

path (Rochim et al., 2017) at least at the laboratory scale, it may be applied to the structure scale of a dam.

Due to the construction phase and to the progressive extraction of the soil from the borrow pit, the material parameters of the dam core are endowed with a spatial variability that cannot be easily reduced (Smith and Konrad, 2011). This spatial variability concerns all material parameters, in particular the hydraulic conductivity, the dry unit weight and the grain size distribution. Logically, it should also affect the erosion resistance index. Hence, it does not seem reasonable to characterize the suffusion susceptibility of such a large structure with only a single value, based on a single laboratory test (Rönnqvist et al., 2014). Rather, a contour map of the erosion resistance index would provide additional valuable information. The objectives of the paper are to assess the suffusion susceptibility of core lifts in zoned dams based on construction data and to locate zones endowed with a relatively larger suffusion potential. To tackle those objectives, a novel approach is presented. This approach is based on four steps, namely (i) the estimation of the erosion resistance index values in the core, (ii) the estimation of the hydraulic conductivities in the core, (iii) the estimation of the power dissipated by the flow in the core, since larger values of the power are related to larger rates of erosion (Marot et al., 2012a) and (iv) the superimposition of the power with the erosion resistance index to locate zones endowed with a relatively larger suffusion potential. This approach was applied to a particular dam as a proof of concept.

## **2. Description of the method**

This section presents a general method to estimate the erosion resistance index and the saturated hydraulic conductivity of core soils from construction data.

## ***2.1. Assessment of soil suffusion susceptibility***

The erosion resistance index of a soil is traditionally obtained by performing an experimental test on a dedicated erodimeter (Marot et al., 2012a, 2016). Yet, soils used in dam cores are characterized by spatial variability that is related to the construction phase and to the intrinsic attributes of the borrow pit. Hence, the characterization of the suffusion susceptibility of core soils would require a large number of erosion tests. To tackle our objective, another approach is proposed based on an existing statistical analysis. Le et al. (2016) conducted suffusion tests on 32 different soils to measure their corresponding erosion resistance index values. The test device and test procedure are demonstrated in Bendahmane et al. (2008). For each experiment, the erosion resistance index  $I_{\alpha}$  was determined at the “final state” (Rochim et al., 2017). From the study of several grain size based criteria, different physical parameters were identified in order to develop a statistical analysis for the prediction of the erosion resistance index. In 1953, US Army Corps of Engineers, proposed to define the stability boundary by the uniformity coefficient  $C_u$ . In greater details, Kenney and Lau (1985) proposed that at each point of the grading curve corresponding to a mass fraction smaller than  $F$  and a particle of diameter  $D$ , the mass fraction  $H$  is measured between particles sizes  $D$  and  $4D$ . The method was proposed based on the original idea that particles of diameter  $D$  may be blocked by pores composed of particles diameter ranging from  $D$  to  $4D$ . The grains smaller than  $D$  can be detached and transported if the soil does not have enough grains within the interval  $D$  to  $4D$ . Two parameters are proposed based on the work of Kenney and Lau (1985), namely  $\min(H/F)$  and *Finer KL*, where  $\min(H/F)$  is the minimum value of  $H/F$  and *Finer KL* is the percentage of finer  $F$  corresponding to  $\min(H/F)$ . Thus, *Finer KL* is a parameter that differentiates the fine particles from the coarse particles and indicates the percentage of fine particles belonging to a soil. Wan and Fell (2008)

proposed a method for assessing internal instability of broadly graded silt-sand-gravel soils. This method is based on two ratios:  $d_{90}/d_{60}$  and  $d_{20}/d_5$  (where  $d_{90}$ ,  $d_{60}$ ,  $d_{20}$  and  $d_5$  are the sieve sizes for which 90%, 60%, 20% and 5% respectively of the weighed soil is finer). More recently, Chang and Zhang (2013) distinguished widely graded and gap graded soils, and they defined  $P$  as the mass fraction of particles finer than 0.063mm. In the case of gap graded soil, they defined the gap ratio as:  $G_r = d_{max}/d_{min}$  ( $d_{max}$  and  $d_{min}$ : maximal and minimal particle sizes characterizing the gap in the grading curve). For low plasticity soils, the percentage of clay but also the mineralogy and the chemical composition of clay characterise soils with a different water sensitivity and a different sensitivity to erosion processes (Haghighi, 2012). In consequence the blue methylene value  $V_{BS}$  is also measured because it permits quite easily and rapidly to highlight the water sensitivity of tested soils. In addition with the grain size distribution, Marot et al. (2012b) showed that the shape of grains also plays an important role on suffusion susceptibility. They used three methods for characterizing grain shape: digital picture analyses, direct shear tests and by gravitating flows with a sand angulometer. Whatever indicator was considered for grain shape characterizing, the same relative classification of the tested aggregates was obtained. However, the measurement of internal friction angle  $\varphi$  under the same density index  $I_d$  ( $I_d = [e_{max} - e]/[e_{max} - e_{min}]$  where  $e_{max}$ ,  $e_{min}$  are the maximum and minimum values respectively of the void ratio  $e$ ) appears to be the more appropriated and easily measured to characterize the influence of the grain shape on the process of suffusion. In a complementary manner with material susceptibility, the stress condition also can influence the suffusion susceptibility. Several tests performed in oedometric conditions on unstable soils showed that a rise in the effective stress causes an increase of the soils' resistance to suffusion (Moffat and Fannin, 2006). In the same manner, when tests were carried out under isotropic confinement (Bendahmane et al.,

2008), the increase in the confinement pressure and then the subsequence local increase of soil density (i.e. smaller size of constrictions between coarse grains) allowed a decrease in the suffusion rate. In this context, the dry unit weight  $\gamma_d$  is also considered. From this review of several parametric studies, fourteen relevant physical parameters were identified: the dry unit weight  $\gamma_d$ , the internal friction angle  $\varphi$ , the Blue Methylene value  $V_{BS}$ , the gap ratio  $G_r$  for gap-graded soil, the percentage  $P$ , the minimum value of  $(H/F)$ , the *Finer KL*, the uniform coefficient of the grain size distribution  $C_u$ , the initial hydraulic conductivity  $k_i$  and  $d_5, d_{15}, d_{20}, d_{50}, d_{60}, d_{90}$ .

First of all, a principle component analysis was conducted to select the main physical parameters and to eliminate the redundant information. Second, by focusing on easily measured parameters and by distinguishing gap-graded soils from widely-graded soils, the multivariate statistical analysis leads to two expressions of the erosion resistance index that involve five physical parameters in total. These parameters represent a given soil activity through the Blue Methylene value  $V_{BS}$ , in a given compaction state through the dry unit weight  $\gamma_d$ . The angularity of the particles is taken into account through the internal friction angle  $\varphi$ . The relevant information issued from the grain size distribution is summarized within the parameters *Finer KL* and  $P$ .

Hence, for widely-graded soils, the following best-fit equation to predict the erosion resistance index for suffusion is proposed:

$$I_\alpha = - 11.32 + 0.45 \gamma_d + 0.20 V_{BS} + 0.10 \varphi + 0.06 \textit{Finer KL} \quad (2)$$

The correlation coefficient  $R^2$  between the prediction and the measurement is 0.93 for the 22 widely-graded specimens. Alternatively, for gap-graded soils, the statistical analysis provides:

$$I_{\alpha} = -20.98 + 0.31 \gamma_d + 5.46 V_{BS} + 0.49 \varphi - 0.13 \text{ Finer } KL - 0.16 P \quad (3)$$

The corresponding correlation coefficient  $R^2$  is 0.93 for the 10 gap-graded specimens. The distinction between widely-graded or gap-graded is based on the gap-ratio  $G_r$  (Chang and Zhang, 2013; Le et al., 2016). Gap-graded soils are defined by  $G_r > 1$ . If this distinction is not obvious, the smallest value of  $I_{\alpha}$  should be taken from the two values calculated by Eq. (2) and Eq. (3) to ensure a conservative estimation.

It should be noted that Eq. (2) and (3) were obtained from soil samples with a full grain size distribution as opposed to scalped (or re-graded) grain size distributions. In the field, it is a common practice to scalp the GSD curve when the maximum particle diameter is really large, so that the in-place maximum grain size is often larger than the maximum grain size used in the laboratory. Yet, the influence of this maximum grain size  $D_{max}$  on the measured internal friction angle  $\varphi$  and *Finer KL* remains an open question.

It may be observed that Eq. (2) uses the parameter *Finer KL* rather than  $P$  to predict the erosion resistance index  $I_{\alpha}$ . This choice is related to the fact that, for widely-graded soils, *Finer KL* is better correlated to  $I_{\alpha}$  than  $P$ . Alternative empirical relations could also be obtained with the parameter  $P$  instead of *Finer KL* or with the angularity instead of the friction angle. In other words, Eq. (2) and (3) may be viewed as resilient tools that can be adapted to the available parameters of a given construction site.

## **2.2. Assessment of the hydraulic conductivity**

The overall hydraulic conductivity of a compacted dam core made of till is in fact an heterogeneous property that reflects the compaction conditions, the progressive construction phases and the intrinsic attributes of the borrow pit (Watabe et al., 2000; Leroueil et al., 2002; Smith and Konrad, 2011). When till is compacted at a water content lower than the optimum value ( $\rho_{opt}$  and  $w_{opt}$ ), corresponding to the current reference

standard Proctor curve, matric suction aggregates the soil particles causing the development of macro porosity, which results in an increased hydraulic conductivity. The till fabric is then considered aggregated. For water contents larger than the optimum, macro porosity is less developed, which results in a lower hydraulic conductivity. The till is then considered homogeneous. To avoid the cumbersome task of performing many permeability tests, several studies succeed in estimating the saturated hydraulic conductivity of glacial till from the fines content and in-situ compaction conditions (Leroueil et al., 2002; Smith and Konrad, 2011; Malenfant-Corriveau, 2016). Leroueil et al. (2002) proposed to predict the saturated hydraulic conductivity of glacial till  $K_{sat}$  (m/s) using an empirical relation based on fines content  $f_{ca}$  and compaction conditions (homogeneous versus aggregated fabric).  $f_{ca}$  is the percentage of the fines content passing  $2\mu\text{m}$  for soil fraction re-graded at  $D_{max}$  equals 5mm, so that sedimentary tests are required to obtain  $f_{ca}$ . Smith and Konrad (2011) proposed to predict the saturated hydraulic conductivity  $K_{sat}$  based on fines content  $f_{cb}$  and compaction conditions (homogeneous versus aggregated fabric).  $f_{cb}$  is the percentage of the fines content passing  $75\mu\text{m}$  for soil fraction re-graded at maximum grain size  $D_{max} = 75\text{mm}$ . This approach is proposed for cases characterized by sedimentary tests conducted during the dam construction. This approach is applicable for fines content  $f_{cb}$  ranging from 25% to 45% for the soil fraction passing 75mm. However, the measured hydraulic conductivity is sensitive to small variations in the fines content  $f_{cb}$  and the data dispersion is somewhat high. Due to the strong nonlinearity between hydraulic conductivity and fines content values, expected values of hydraulic conductivity inferred from the fines content will present a bias (Smith and Konrad, 2011). Therefore, compared to the method proposed by Leroueil et al. (2002), the method proposed by Smith and Konrad (2011) is less precise, however, useful for cases when sedimentary tests are not available.

Both studies (Leroueil et al., 2002; Smith and Konrad, 2011) have proposed two empirical relations that account for the influence of the till's fabric, i.e. aggregated or homogeneous. However, the laboratory studies of Malenfant-Corriveau (2016) showed that the saturated hydraulic conductivities for some tills endowed with a low percentage of fines content passing  $2\mu\text{m}$  (0.7% for the fine fraction passing  $D_{max} = 5\text{mm}$ ) do not depend on the fabric of the soil. The study was conducted on eleven specimens compacted at different water contents. It shows that the saturated hydraulic conductivity  $K_{sat}$  is similar for the specimens compacted on the dry side and on the wet side of the optimum. The measured hydraulic conductivities remain in the same order of magnitude ( $10^{-7}\text{m/s}$ ). Since the hydraulic conductivity is strongly related to the microstructure of the soil, the authors conclude that the eleven specimens have similar soil structures which may be attributed to the low percentage of fines content passing  $2\mu\text{m}$ .

Malenfant-Corriveau (2016) proposed to predict the saturated hydraulic conductivity  $K_{sat}$ , at the temperature of  $20^\circ\text{C}$ , based on the modified Kozeny-Carman equation which can cover those particular tills endowed with a low percentage of fines content:

$$\begin{aligned}
 K_{sat} &= 0.024622 \alpha^{0.7825} & \alpha \geq 0.01\text{mm}^2 \\
 K_{sat} &= 0.1264 \alpha^{1.1377} & \alpha < 0.01\text{mm}^2
 \end{aligned} \tag{4}$$

Here, the parameter  $\alpha$  (Chapuis, 2004) is expressed as a function of the porosity  $n$  and  $d_{10}$  (the effective diameter for the soil fraction re-graded at  $D_{max}$  equals to 5 mm):

$$\alpha = d_{10}^2 \frac{n^3}{(1-n)^2} \tag{5}$$

Note that the parameter  $\alpha$  is expressed in  $\text{mm}^2$  in both Eq. (4) and (5).  $d_{10}$  can be obtained based on sedimentary test, and the porosity  $n$  can be obtained based on in-situ density measurements:

$$n = \frac{w \rho}{(1+w) \rho_w S_r} \quad w = \frac{\rho - \rho_d}{\rho_d} \quad S_r = \frac{\rho - \rho_d}{\left(1 - \frac{\rho_d}{\rho_s}\right) \rho_w} \quad (6)$$

where  $w$  is the water content,  $\rho$  is the wet density,  $\rho_w$  is the density of water,  $S_r$  is the saturation ratio and  $\rho_s$  is the solid density. Therefore to predict the saturated hydraulic conductivity for each specimen, the required data include the effective diameter  $d_{10}$  and the in-situ wet and dry densities.

All three approaches (Leroueil et al. (2002), Smith and Konrad (2011) and Malenfant-Corriveau (2016)) can be used to estimate the saturated hydraulic conductivity of till soils. The best choice depends first on the nature of the material: the percentage of fines content. If the material fits the range of validity of several methods, the best choice depends next on the required data. Moreover, likewise  $D_{max}$  might influence the estimation of *Finer KL*, one should have in mind that  $d_{10}$  is dependent of the cut-off  $D_{max}$ , when using Eq. (4) and (5).

## ***2.2. Assessment of the relative suffusion potential***

It is worth emphasizing that  $I_\alpha$  is just a material parameter that characterizes the susceptibility of a given soil to suffusion. Hence, it cannot be interpreted as a “security factor” to distinguish between “probable occurrence of erosion” and “no erosion”. This distinction requires additionally the estimation of the hydraulic loading.

The hydraulic loading on the grains is often described by three distinct parameters: the hydraulic gradient, the hydraulic shear stress and the pore velocity. However, the

filtration of some detached particles can induce a clogging process within the soil accompanied with the decrease in the hydraulic conductivity (Marot et al., 2016). Therefore, variations of both seepage velocity and hydraulic gradient (or pressure gradient) have to be taken into account to evaluate the hydraulic loading. With such objective, the hydraulic loading can be expressed in terms of the power expended by the seepage flow  $P_{flow}$ . The estimation of  $P_{flow}$  for each lift requires as input the pressure field, the elevation and the hydraulic conductivity. The pressure field can either be estimated from simplified boundary conditions, or can be precisely computed with a FEM simulation.

As a consequence, the relative suffusion potential of the dam core may be characterized by the contour maps of the erosion resistance index  $I_\alpha$  and that of the power dissipated by the flow  $P_{flow}$ . The first contour map informs on the suffusion susceptibility of the till core. It may give an idea of the homogeneity of this suffusion susceptibility and it may point out zones endowed with a low resistance to suffusion. It represents a first attempt to apply the energy approach at dam-scale. The second contour map informs on the hydraulic load within the till core.

The combination of the two contour maps and in particular the superimposition of zones characterized by a relatively lower suffusion resistance index and a relatively larger power dissipated by the flow may be a first attempt to identify zones characterized by a greater suffusion potential. Although, the erosion resistance index  $I_\alpha$  by itself is only a material parameter which cannot describe the kinetic of the erosion process, one may infer that the combination of lower  $I_\alpha$  and larger  $P_{flow}$  would target zones endowed with a greater suffusion kinetic. This combination represents a first effort to tackle the question ‘Where, inside a large volume, do we have a relatively larger suffusion potential?’.

### 3. Application to a particular dam

#### 3.1. Description of the dam

The analyzed dam is a 90m high, 300m wide and 447m long hydraulic structure founded on bedrock foundations. The dimensions of the dam and the location of each sample taken from the dam are characterized by *PM*, *ecart* and *elevation* for longitudinal, transversal and vertical direction, respectively.

A cross section view of the dam at its highest section ( $PM = 330\text{m}$ ) is shown in Fig. 1. This zoned dam is composed of a central impervious core (zone 1), a downstream filter (zone 2A), an upstream filter (zone 2B) and rockfill (zones 3A, 3B, 3C, 3D and 3E). The crest level is 368m and the maximum reservoir level is 366.3m.

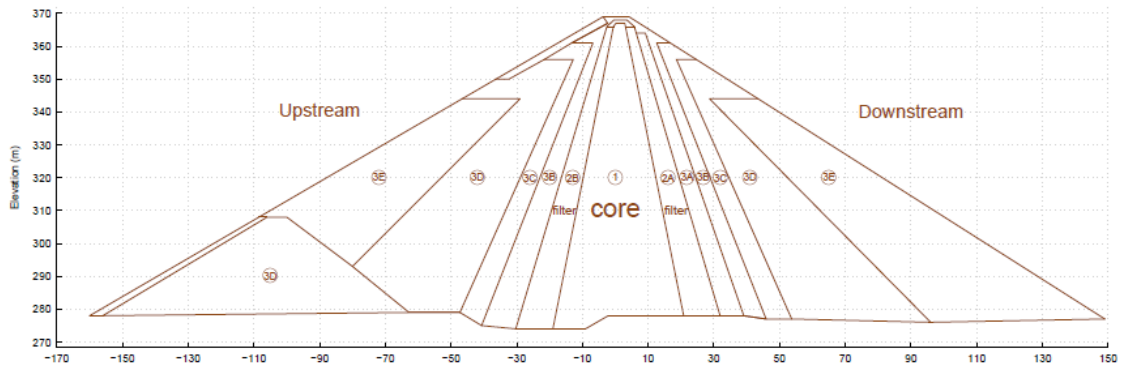


Figure 1. Cross section of the analysed dam at its maximum height ( $PM = 330\text{ m}$ ).

The central impervious core is made of compacted, low plasticity glacial till from Northern Québec. The till is a well-graded soil which maximum particle size is up to 300mm. The grain size distribution generally becomes coarser from the central core to the rockfill. The glacial till used to build the core comes from a preselected nearby borrow pit. The placement of the till was realized by dumping and spreading the material in lifts across the entire width of the core.

The dam may be characterized with heterogeneities in terms of soil physical properties, such as porosity, hydraulic conductivities. Construction control tests and measurements (laboratory and in-situ measurements) were conducted to obtain grain size distributions, water contents and density values at various sampling points.

The sampled data from the dam include full grain size distributions (0.001mm - 300mm), partial grain size distributions or sieve tests (0.08mm - 80mm), densities, water contents, degrees of compaction and degrees of saturation. The longitudinal view and cross section view of the locations of the soil specimens are shown in Fig. 2. The sample locations used for sedimentary tests are shown in Fig. 2(a) and (b); while that used for in-situ density measurements, sieve tests and proctor tests are shown in Fig. 2 (c) and (d). It can be seen that the number of sedimentary tests is lower than the number of in-situ density measurements.

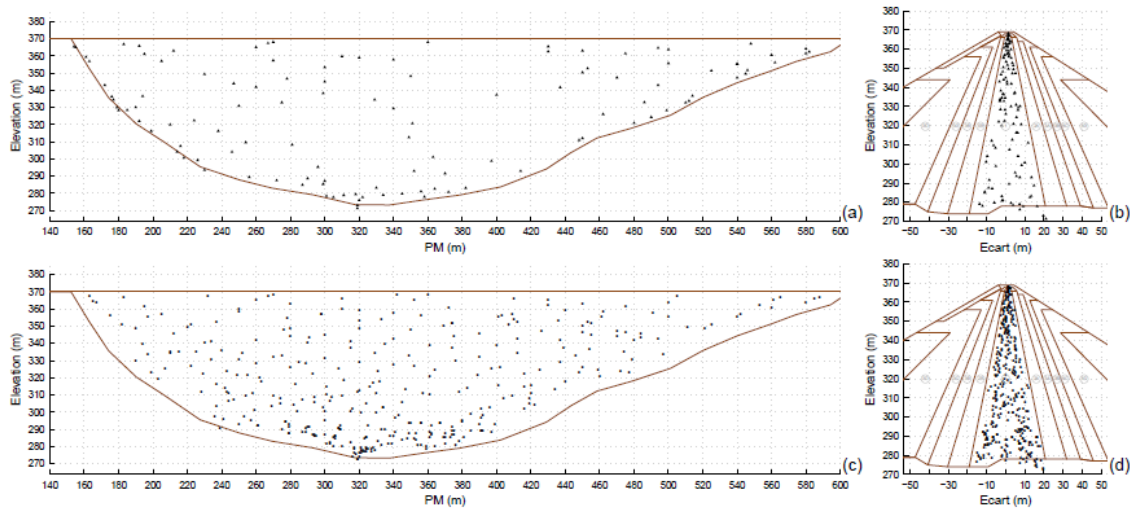


Figure 2. (a) Longitudinal view and (b) cross section view of sample locations used for sedimentary tests; (c) longitudinal view and (d) cross section view of sample locations used for in-situ density measurements, sieve tests and proctor tests.

Based on the grading of the part of the till finer than 4.75mm, the percentage of fine fraction passing 0.075mm lies within 22.6% and 39.2%. Therefore  $D_{15F}$  should be lower than  $D_{15F} < [0.80\text{mm}, 4.60\text{mm}]$  to respect the filter criterion proposed by Sherard

and Dunnigan (1989). The maximum allowed size of  $D_{15F}$  for filters is 0.7mm, which confirms that the downstream filter fulfills the basic filter criterion based on the grain size distributions. Complementary experimental tests could be conducted to evaluate the influence of the compatibility between the soil and the filter, for instance the continuing erosion filter test (Foster, 2007).

### ***3.2. Estimation of the erosion resistance index***

For the particular dam at hand, the estimation of erosion resistance index is based on Eq. (2) since all soil samples are widely-graded. Cautiously, prior to the extensive use of this approach to the entire dam, an experimental validation has been performed by Le (2017). The result of this suffusion experiment realized on a till sample taken from this particular dam has been compared with the estimation issued from the statistical analysis. The till soil was sieved at  $D_{max}$  equals 5mm. The internal friction angle for the sieved till measured  $37^\circ$ , the Blue Methylene value was 0.7g/100g and the dry unit value was 19.14 kN/m<sup>3</sup>. The erosion resistance index obtained from the suffusion experiment equals 5.76, which is very close to the predicted value using Eq. (2) based on the statistical analysis (5.72). Therefore, this suffusion test validates the use of Eq. (2) for till samples taken from the dam.

Among the four soil parameters of Eq. (2), two were considered constant throughout the core, namely the Blue Methylene value  $V_{BS}$  and the internal friction angle  $\varphi$ . This simplification is introduced because no dedicated measurements were realized during the construction. As mentioned before, the internal friction angle used to estimate the erosion resistance index  $I_\alpha$  is introduced to describe the angularity of soil particles rather than the failure envelope of the soil under shearing. In fact, till is a fractal material which means that the particle's angularity is not influenced by the particle's size. Besides,

the till at hand is a non-plastic material, i.e. it is associated with a really low value of  $V_{BS}$ . Finally, the till is progressively extracted from a single borrow pit, so that one may reasonably assume that  $\varphi$  and  $V_{BS}$  are uniform within the whole dam. The Blue Methylene value was estimated at a constant value of  $V_{BS0} = 0.49\text{g}/100\text{g}$  (70% of the value presented above which was measured on a soil sieved at 5mm), which is now representative of the full grain size distribution, i.e. the in-place till soils. The internal friction angle is in turn estimated to  $\varphi_0 = 37^\circ$  (same as that of the sieved soil).

Regarding the two other parameters of Eq. (2), i.e. the dry unit weight  $\gamma_d$  and *Finer KL*, their spatial variabilities are now estimated based on the available construction data (see Fig. 2) and investigated by plotting their corresponding contour maps.

### *3.2.1. Spatial variability of dry unit weight $\gamma_d$ in the dam core*

The methodology used to obtain the contour map of the dry unit weight for the whole dam core is presented below as an example. The spatial variabilities of other soil parameters are investigated following the same approach.

First, 349 measurements of dry unit weight values were selected from the dam core (samples located at the contact zone between the dam core and the bedrock boundaries are not considered) and presented in histogram plot (Fig. 3). The histogram plot is divided into eight intervals which covers the  $\gamma_d$  values from the minimum to the maximum. The width of each interval equals the standard deviation of the 349 set of  $\gamma_d$  values. Each interval is assigned with a specific color to cover the ranged values. Fig. 3 indicates that the  $\gamma_d$  values are approximately normally distributed.

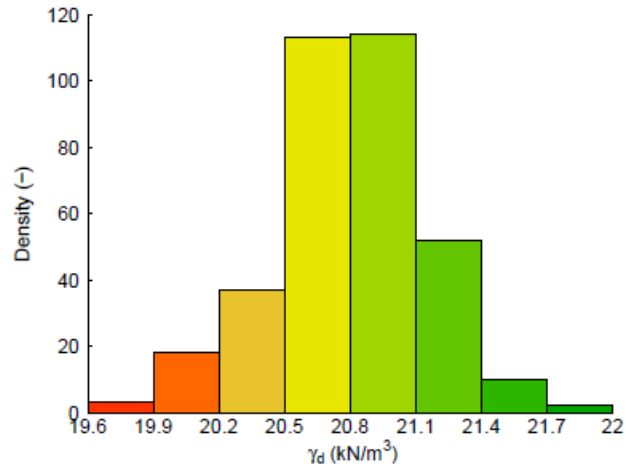


Figure 3. Histogram plot of 349 measured dry unit weight values.

Second, since the placement of the till during the construction was realized by dumping, spreading and compacting the material in lifts of 0.45m height across the entire width of the core, the dam core was divided into sublayers of 0.45m height to account for the construction procedure. As a result, a total of a priori 212 different sublayers is identified to start with. Likewise in Fig. 2(b) and (d), all the 349 points used for dry density measurements are plotted in the section view in Fig. 4(a) regardless of their *PM* position. Therefore, each sublayer is characterized with several or zero dry density measurements. For each sublayer endowed with at least one measurement, an average value is computed and a corresponding color/interval is assigned (same color as defined in Fig. 3). For sublayers without any measurements available, a null value is assigned, see Fig. 4(a). Therefore, only the vertical variability of the dry unit weight is taken into account.

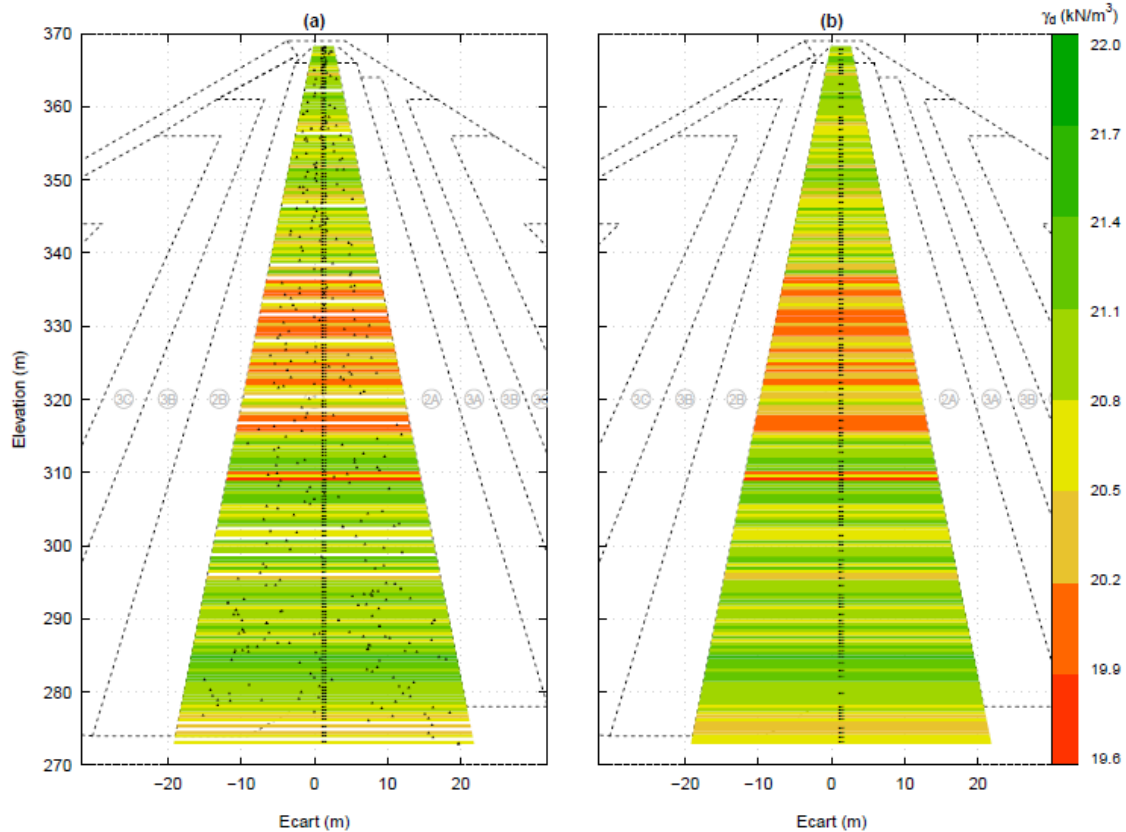


Figure 4. Contour maps of the dry unit weight  $\gamma_d$  for (a) 212 sublayers of 0.45 m height and (b) 150 layers after the smoothing technique

Third, a smoothing technique was used to reduce the number of layers. When several adjacent sublayers are characterized by the same color interval, the sublayers are combined to define a new smoothed layer whose thickness equals the sum of these sublayers' thickness. The new smoothed layer is assigned with an average value computed from all the data of the adjacent sublayers and with an interval color according to the new averaged value. For sublayers characterized with zero measurement, a conservative estimation is proposed: the sublayer takes the conservative value from the adjacent upward and downward non-zero average values. This approximation relies on the fact that two adjacent sublayers come from the same spatial zone within the borrow pit and share the same properties. For the dam at hand, all sublayers having a null value of dry density are adjacent to sublayers having non-zero values (Fig. 4(a)). As a result, a

total of 150 new smoothed layers is obtained with this smoothing technique, see Fig. 4(b). The spatial variability of the dry unit weight  $\gamma_d$  ranges from 20-22kN/m<sup>3</sup> in most of the core, except within the elevations between 315m to 335m that are characterized with slightly lower values (19.6-20kN/m<sup>3</sup>). Those results illustrate the consistency and the good quality of the compaction methodology.

### 3.2.2. Spatial variability of *Finer KL* in the dam core

The calculation of *Finer KL* requires a priori the full grain size distribution of each soil sample (1 $\mu$ m - 300mm), while for the whole dam, only 33 samples whose full grain size distributions are available, the most available data lies within 80 $\mu$ m - 80mm (sieve tests, Fig. 2 (c) and (d)). To alleviate this constraint, the influence of the cut-off  $D_{max}$  on the parameter *Finer KL* was investigated.

(i) In a first step, one representative till specimen, with its full grain size distribution, was selected to investigate the effects of the cut-off  $D_{max}$  on the variation of *Finer KL* (Fig. 5). The grain size distribution curves are plotted for three values of  $D_{max}$ : 5mm, 80mm and 300mm. For the scalped curves, the coarse material that has been removed, respectively 5mm - 300mm and 80 - 300mm was not replaced. Fig. 5(b) indicates that for this particular soil, the parameter *Finer KL* (the percentage F corresponding to the minimum of H/F) is larger than 80% regardless of the cut-off values; therefore, *Finer KL* is mainly determined by the coarse fraction. Moreover, the influence of  $D_{max}$  on *Finer KL* for this soil is observed to be fairly low. (ii) The previous methodology is applied to 33 soils from the dam core whose full grain size distributions are available.

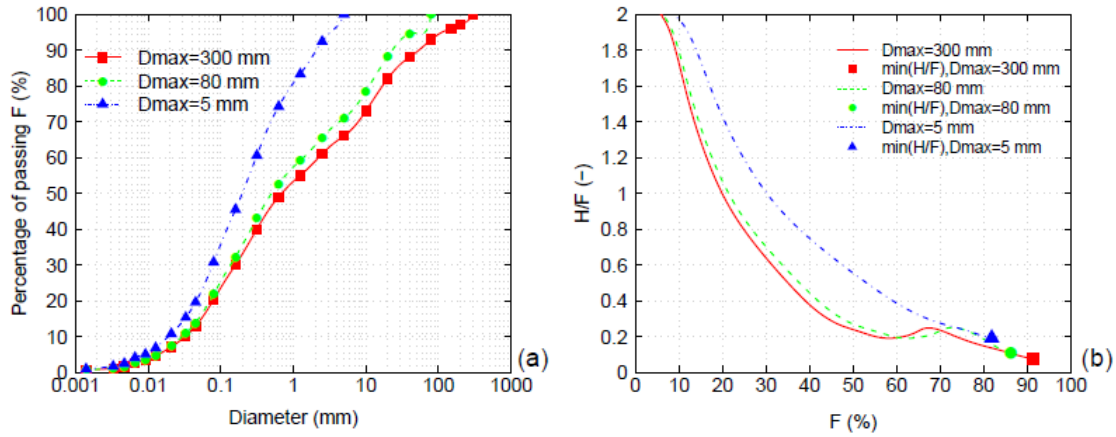


Figure 5. For one particular soil: (a) Grain size distribution curves of one representative specimen for cut-off  $D_{max}$  at 300 mm, 80 mm and 5 mm, respectively; (b) The corresponding evolution of  $H/F$  with fine fraction  $F$ .

The average value of *Finer KL* decreases slightly from 86% to 82% with decreasing value of  $D_{max}$ . Hence, using a GSD curve scalped at  $D_{max}$  equals 80mm induces a slight underestimation of the averaged value of *Finer KL*, which further induces a conservative estimation of the erosion resistance index  $I_{\alpha}$ , see Eq. (2). Also, data corresponding to small diameters (1 $\mu$ m - 80 $\mu$ m) are not required to estimate *Finer KL*. As a conclusion, the estimation of *Finer KL* does not require a full grain size distribution for this particular soil, so that sieve tests (80 $\mu$ m - 80mm) may be used to estimate the parameter *Finer KL*. This conclusion will permit to take advantage of the numerous sieve tests presented in Fig. 2 (c) and (d). 391 measured *Finer KL* values based on  $D_{max} = 80$ mm are plotted in the form of a histogram plot (Fig. 6).

The results indicate that only 10% of the *Finer KL* values are smaller than 80%, the other values are all larger than 80% and are approximately normally distributed. Following the same methodology as the one presented in section 3.2.1, the spatial variability of *Finer KL* is presented in Fig. 7 (a). A total of 122 smoothed layers is obtained. Most of the layers are characterized by *Finer KL* values larger than 70% except

several layers at elevations of 283.5m, 315.5m and 318m. Those results illustrate the intrinsic properties of the borrow pit that have been slightly shuffled by the construction procedure.

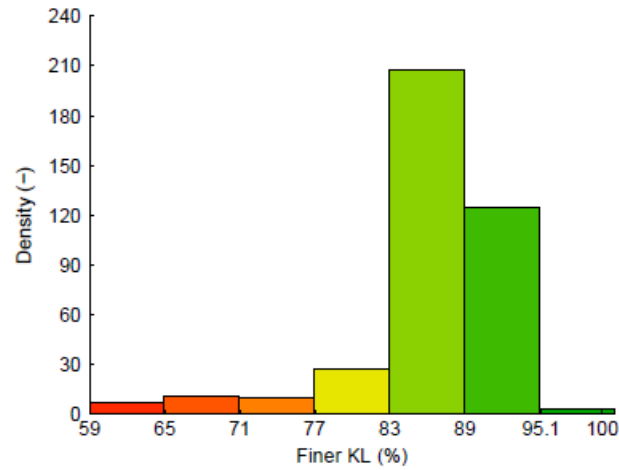


Figure 6. Histogram plot of 391 measured *Finer KL* values based on  $D_{max}$  equal 80mm

### 3.2.3. Spatial variability of the erosion resistance index $I_\alpha$ in the dam core

The spatial variability of the erosion resistance index  $I_\alpha$  in the dam core is investigated by plotting the contour map of  $I_\alpha$ . The spatial distribution of  $I_\alpha$  is predicted based on Eq. (2) by taking into account the spatial variabilities of  $\gamma_d$  presented in Fig. 4(b) and *Finer KL* presented in Fig. 7(a).

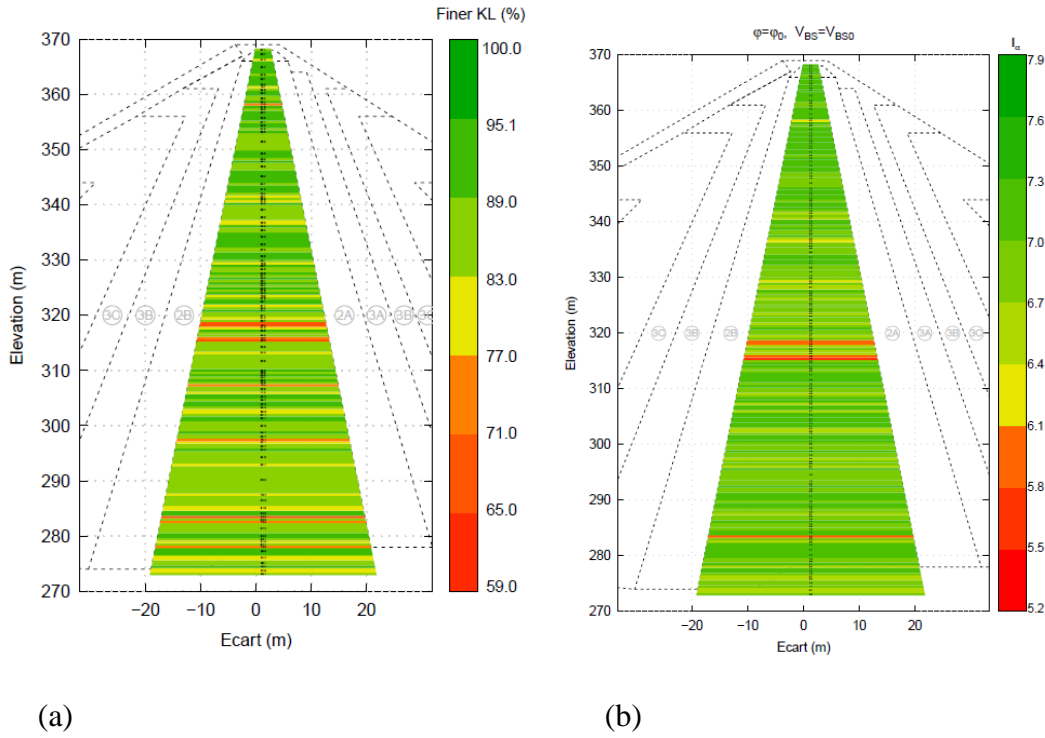


Figure 7. Contour map of: (a) *Finer KL* after the layer smoothing technic and (b) the predicted erosion resistance index  $I_\alpha$

The internal friction angle and Blue Methylene values were considered constant for the whole dam core,  $\varphi = \varphi_0 = 37^\circ$  and  $V_{BS} = V_{BS0} = 0.49\text{g}/100\text{g}$ . Therefore, the number of  $I_\alpha$  layers is defined by combing the smoothed  $\gamma_d$  layers and *Finer KL* layers. Each layer of  $I_\alpha$  is related to a unique value of  $\gamma_d$  and *Finer KL*. Hence, the number of  $I_\alpha$  layers is larger than that of  $\gamma_d$  layers alone or *Finer KL* layers alone. No smoothing technique was used to improve the  $I_\alpha$  contour map, so that no artificial values of  $I_\alpha$  are computed for layers associated with zero measurement of  $\gamma_d$  and *Finer KL*. The contour map of the erosion resistance index  $I_\alpha$  is shown in Fig. 7(b).

The predicted values of  $I_\alpha$  lie within the range of 5.6 to 7.3. The dam core appears to be fairly homogeneous and the layers are mainly characterized as highly resistant to suffusion ( $I_\alpha \geq 6$ ), except for two zones near the elevations 315.6m and 318.3m that are

characterized as resistant to suffusion due to the relatively lower erosion resistance index values ( $5.6 < I_{\alpha} < 6$ ) (Marot et al., 2016).

So far, when investigating the spatial variation of the erosion resistance index, two parameters have been considered constant for the whole dam core, namely the internal friction angle  $\varphi$  and the Blue Methylene value  $V_{BS}$ . These values originate from a single sample, so that the natural variability of those soil parameters has been neglected. According to Phoon and Kulhawy (1999), the coefficient of variation for the internal friction angle  $\varphi$  ranges between 5% and 10% for good quality and direct measurements. Therefore, a sensitivity analysis is proposed to investigate the influence of the internal friction angle  $\varphi$  and of the Blue Methylene value  $V_{BS}$  on the erosion resistance index.

With all the other parameters kept constant ( $\gamma_d$  takes the values presented in Fig. 4(b), *Finer KL* takes the values presented in Fig. 7(a) and  $V_{BS} = V_{BS0} = 0.49\text{g}/100\text{g}$ ), the erosion resistance index is calculated for three values of the internal friction angle,  $33.3^\circ$ ,  $37^\circ$  and  $40.7^\circ$ , which correspond to 90%, 100% and 110% of  $\varphi_0$ , respectively (Fig. 8). The comparison indicates that  $\varphi$  has an important influence on the erosion resistance index. Therefore, one way to improve the actual state of practice would be to account for the variability of the in-place internal friction angle rather than taking a single value for the whole dam.

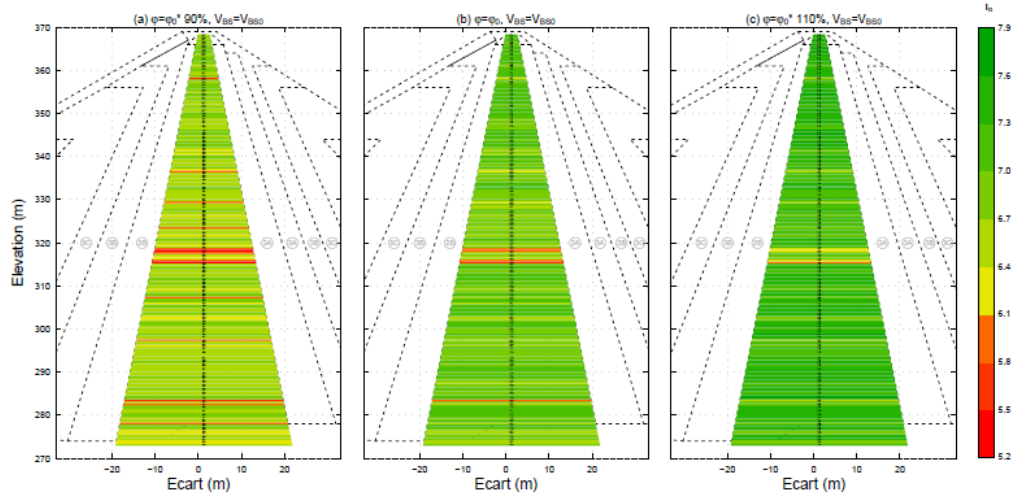


Figure 8. Contour maps of the erosion resistance index  $I_\alpha$  by taking boundary values of the internal friction angle corresponding to (a) 90%, (b) 100%, (c) 110% of  $\varphi_0$ , respectively

Likewise, with all the other parameters kept constant ( $\gamma_d$  takes the values presented in Fig. 4 (b), *Finer KL* takes the values presented in Fig. 7(a) and the internal friction angle  $\varphi = \varphi_0 = 37^\circ$ ), the erosion resistance index is calculated for three values of  $V_{BS}$ , 0.47g/100g, 0.49g/100g and 0.51g/100g, which correspond to 95%, 100% and 105% of  $V_{BS0}$ , respectively (Fig. 9).

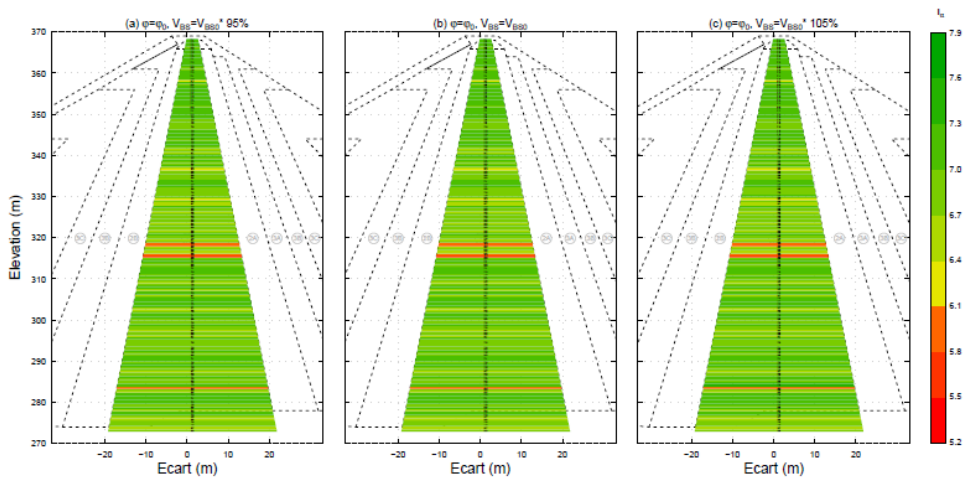


Figure 9. Contour maps of the erosion resistance index  $I_\alpha$  by taking boundary values of the Blue Methylene value corresponding to (a) 95%, (b) 100% and (c) 105% of  $V_{BS0}$ , respectively

The results indicate that the variation of  $V_{BS}$  has very little influence on the erosion resistance index. Hence, for this particular non-plastic till, the systematic measurement of  $V_{BS}$  on each sample is not required to obtain a good estimation of the erosion resistance index. It should be noted that this conclusion may not be generalized to other type of soils.

### ***3.3. Estimation of the saturated hydraulic conductivity***

Investigations on the till used to build the dam at hand indicate that the till contains a very low percentage of fine passing 2mm (the average fines content percentage is 1% for the fraction passing 5mm). Thus, for this particular dam, the approach of Malenfant-Corriveau (2016) is more suitable than the approach of Leroueil et al. (2002). In addition, sedimentary tests are available for this dam so that the approach of Malenfant-Corriveau (2016) is favored in front of the approach proposed by Smith and Konrad (2011) for accuracy reasons. This choice is validated by the laboratory measurement with  $10^{-7}$  m/s, that is better predicted by the method of Malenfant-Corriveau (2016) with  $10^{-7}$  m/s than by that of Smith and Konrad (2011) with  $6.4 \cdot 10^{-6}$  m/s.

According to Eq. (5) and (6), the effective diameter  $d_{10}$  and the porosity  $n$  of the soils are required. Now, remember that the correlation proposed by Malenfant-Corriveau (2016) is based on cut-off samples at  $D_{max} = 5$  mm, while the maximum particle size of the core soils is up to 300 mm. This gap highlights the assumption that the hydraulic conductivity is controlled by the smaller particles of the full GSD. Although reasonable, to date no experimental study can confirm or invalidate this assumption.

The prediction of the spatial variability of  $K_{sat}$  requires the spatial variability of both the effective diameter  $d_{10}$  and of the porosity  $n$ . The measurement of  $d_{10}$  requires a sedimentary test which needs more time to perform in practice. This explains that the number of sedimentary tests is limited to 115 for the whole dam. On the other hand, more density measurements are available to compute the porosity  $n$ . The calculation of the porosity  $n$  for each point follows Eq. (6) with the solid density  $\rho_s = 2720 \text{ kg/m}^3$  (Smith, 2000). A total of 352 porosity values are obtained based on the selected in-situ density measurements in the dam core. The histogram plot of  $d_{10}$  and  $n$  are plotted in Fig. 10.

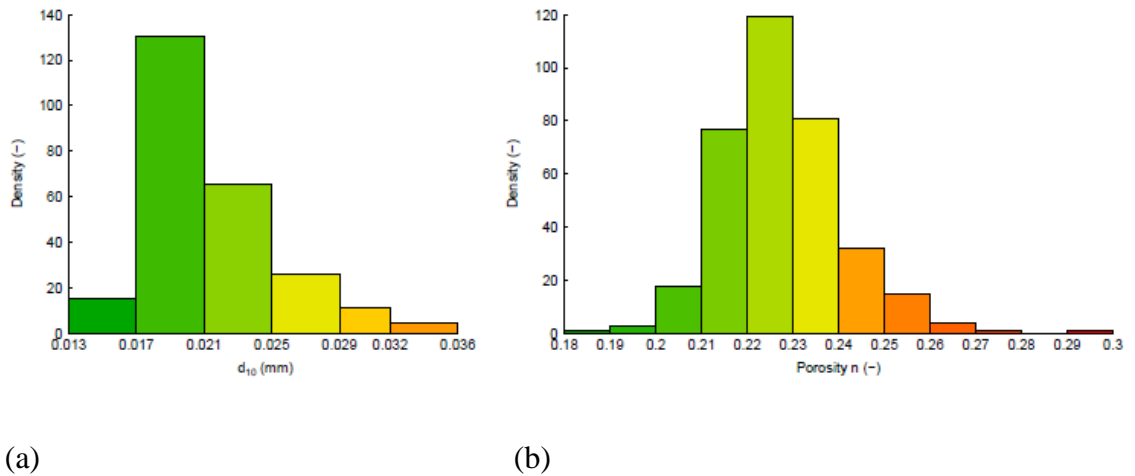
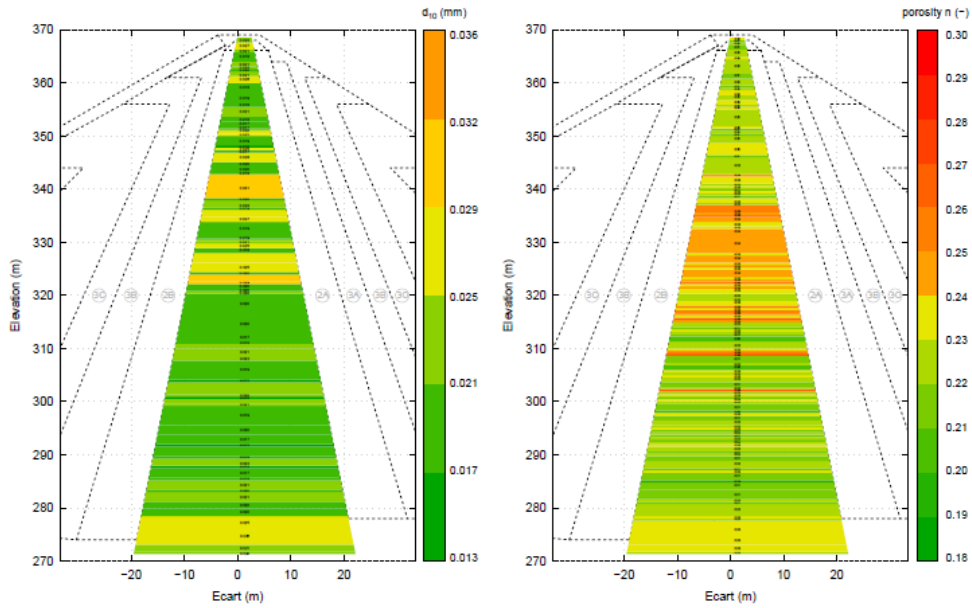


Figure 10. Histogram plots of (a) 115 effective diameter  $d_{10}$  values measured from sedimentary tests and (b) 352 porosity values based on in-situ density measurements

The set of porosity values appears closer to a normally distributed curve than the set of  $d_{10}$  values issued from the grain size distribution of till samples. In fact those discrepancies reflect the intrinsic variability of the soil due to the progressive extraction from the borrow pit and the rather regular compaction procedure. The same observation stands for  $\gamma_a$  and *Finer KL*.

Following the same methodology as that presented in section 3.2.1, the spatial variabilities of the effective diameter  $d_{10}$  and of the porosity  $n$  are shown in Fig. 11.



(a)

(b)

Figure 11. Contour maps of: (a) the effective diameter  $d_{10}$  and of (b) the porosity  $n$  in the dam core

The results indicate that heterogeneities of  $d_{10}$  and porosity  $n$  exist. The spatial variation of the porosity  $n$  is correlated with the spatial variability of the dry unit weight as presented in Fig. 4(b). Two dam zones, namely the zone within the elevation between 320m and 345m as well as the contact zone between the dam and the bedrocks near the elevation of 275m, are characterized with relatively larger values of  $d_{10}$  and larger values of porosity  $n$ .

Finally, following the same methodology as presented in section 3.2.3, the spatial variability of the predicted saturated hydraulic conductivities of the till is obtained based on the smoothed contour map of the effective diameter  $d_{10}$  and that of the porosity  $n$ . A total of 164 layers for the saturated hydraulic conductivity are obtained (Fig. 12). Overall, the hydraulic conductivity distribution is found to be reasonably homogeneous within the range of  $0.6 \cdot 10^{-7} \text{m/s}$  and  $6.8 \cdot 10^{-7} \text{m/s}$ . The predicted hydraulic conductivities fulfill not only the practical requirements ( $< 10^{-6} \text{m/s}$ ) but are also consistent with the laboratory

measurements (Malenfant-Corriveau, 2016). Slightly larger values of  $K_{sat}$  ( $> 5 \cdot 10^{-7} \text{m/s}$ ) are predicted in zones near the central parts of the core within the elevations between 322m and 342m.

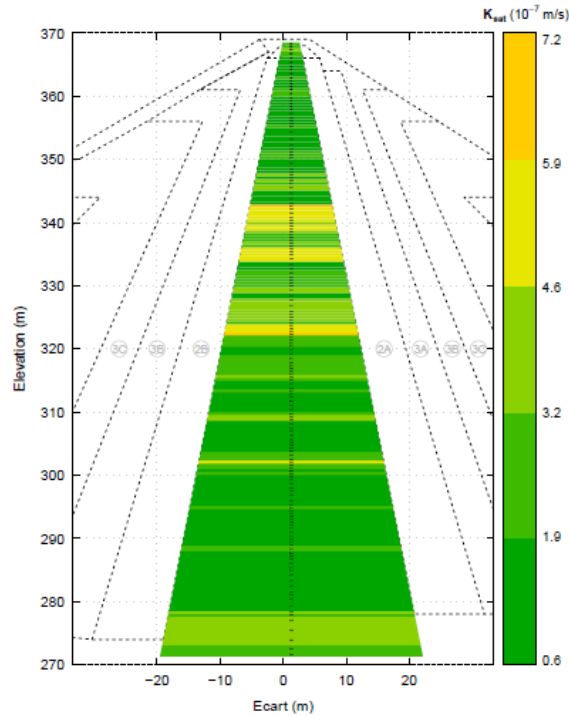


Figure 12. Contour map of the predicted saturated hydraulic conductivity  $K_{sat}$

The proposed estimation of the hydraulic conductivity does not take into account the rather cold temperature of the water ( $5^{\circ}\text{C}$ ) at the dam location. This temperature tends to increase the water dynamic viscosity compared with the laboratory experiments performed at  $20^{\circ}\text{C}$  and hence to decrease slightly our estimation of the hydraulic conductivity. In addition, although our estimation of the hydraulic conductivity is precise enough to estimate the power dissipated by the flow, further studies will be developed to improve the estimation of the hydraulic conductivity.

### ***3.4. Estimation of the suffusion potential***

Based on the obtained contour map of hydraulic conductivities, the powers dissipated by

the flow  $P_{flow}$  are evaluated for each core layer. The method to compute  $P_{flow}$  within each layer is based on a simplified pressure field. Three assumptions are used: (1) no loss of hydraulic head is accounted for in the dam materials upstream of the till core, (2) the fluid pressure is assumed equal to the atmospheric pressure all along the downstream side of the till core and (3) the flow within the core is assumed horizontal in the transversal direction. By using those three assumptions,  $P_{flow}$  within each layer is expressed by:

$$P_{flow} = \frac{K_{sat} \gamma_w h_w^2 S}{L_{AB}} \quad (7)$$

where  $\gamma_w$  is the weight of water,  $h_w$  is the water head,  $S$  is the layer section along  $PM$ , and  $L_{AB}$  the layer longitudinal length.

Following Eq. (7), the spatial distribution of  $P_{flow}$  in the dam core is presented in Fig. 13(b), the unit of [ $10^{-4}$  W] is due to the large dispersion of the  $P_{flow}$  values (the maximum power is 1.42 W, which is 5 orders of magnitude larger than the smallest non-zero value). The spatial discretization of the core into layers for  $P_{flow}$  is the same as that of the hydraulic conductivity, so that  $P_{flow}$  share the same layer thickness and layer number as that of hydraulic conductivity.

The contour maps of the power dissipated by the flow and of the erosion resistance index ( $\varphi = 37^\circ$ ,  $V_{BS} = 0.49\text{g}/100\text{g}$ ) are plotted next to each other for correlation purpose (Fig. 13b).

Areas with a lower erosion resistance index than the average value of 6.95 point towards zones that are more sensitive to suffusion. Dam layers near the elevations 326m, 303m and elevations below 288m are characterized with powers larger than the average value of 0.14 W. The combination of these two results shows that for zones around elevations 329.4m, 318.5m, 315.5m, 302.5m, 296m, 283.5m, 278m, 276 m, the powers dissipated by the flow are relatively large and the erosion resistance indexes have

relatively lower values. The occurrence of these two characteristics highlights zones with a relatively larger suffusion potential, compared with other zones within the dam core. Thus the combination of the spatial variability of both the power dissipated by the flow and the erosion resistance index, is a first attempt to assess the spatial variability of the suffusion potential within the dam core. The main advantage of this approach is that it accounts for both the soil physical characteristics and the construction process.

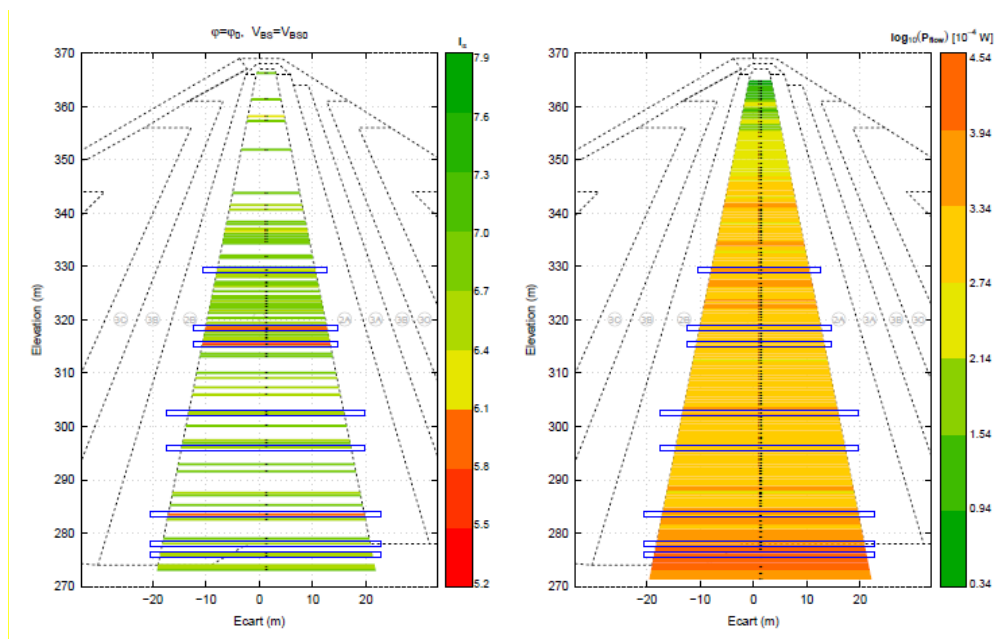


Figure 13. Contour maps of: (a) the predicted erosion resistance index for layers characterized with values smaller than the average value of 6.95 ( $\varphi = \varphi_0 = 37^\circ$ ,  $V_{BS} = V_{BS0} = 0.49$  g/100g) and (b) the predicted power dissipated by the flow. Layers endowed with both relatively smaller  $I_\alpha$  and larger  $P_{flow}$  values are highlighted with blue boxes

This combination represents a first effort to assist dam stakeholders in identifying zones that may require a specific monitoring with respect to suffusion. One limitation is that the stress state of dam layers is not considered. The correlation between the confining pressure and the suffusion susceptibility is to-date not clear. Contradictory results can be found, such as Bendahmane et al. (2008), Chang and Zhang (2013), Ke and Takahashi

(2014), Le et al., (2017), Tomlinson and Vaid (2000). Therefore, these conclusions cannot be generalized. Nevertheless, the dry densities used to estimate the erosion resistance index  $I_\alpha$  for the dam soils come from in-situ measurements during the construction process. We expect that these dry densities will increase after construction due to consolidation, so that the estimation of  $I_\alpha$  is quite conservative, which ensures a safety allowance. Additional work should be done to account for the effects of effective stress and to predict the kinetic of the suffusion process over the dam's lifetime.

In the case of non-plastic soils, the process of concentrated leak erosion may not appear. However if the downstream filter is poorly designed or cracked, the occurrence of backward erosion process should be considered. This case could be studied by using the empirical relationship between physical parameters and the erosion resistance index for interface erosion (Regazzoni and Marot, 2011). Finally for considering the case of contact erosion, additional work should be realized to take into account the seepage length effect.

#### **4. Conclusion**

The aim of this paper was to present a method to investigate the preliminary dam safety in terms of suffusion, based on the spatial distributions of the erosion resistance index  $I_\alpha$ , the saturated hydraulic conductivity  $K_{sat}$  and the power dissipated by the flow  $P_{flow}$  within the dam core. The method was applied to a particular dam of Northern Québec. For this particular dam, the erosion resistance index values  $I_\alpha$  were estimated using an empirical relationship obtained from a statistical analysis. This relation involves the dry unit weight, the Blue Methylene value, the friction angle and the *Finer KL* parameter. This relation has been validated for the studied dam till by comparing the estimated value with a

suffusion test result. On one hand, the Blue Methylene value and the friction angle were considered as constant parameters. On the other hand, the contour of the dry unit weight and the *Finer KL* parameter were computed to account for the till deposition process and for the progressive extraction of the soil from the borrow pit, respectively. The inferred values of the erosion resistance index are between 5.6 and 7.3 which characterise soils resistant and highly resistant to suffusion. For this particular dam, the hydraulic conductivities were inferred using a modified Kozeny-Carman equation. This relation involves the porosity and the effective diameter  $d_{10}$ . The contour map of the porosity is related to the in-situ measured wet density and dry density and hence accounts for the compaction conditions. The contour map of effective diameter  $d_{10}$  is inferred from sedimentary tests and reflects the progression of till placement during construction. The predicted values of hydraulic conductivities are within the order of magnitude  $10^{-7}$  m/s, which is consistent with laboratory measurements. Overall, the hydraulic conductivities appear fairly homogeneous and fulfill the practical requirements.

Based on the in-place hydraulic conductivities and on simplified pressure boundary conditions, the power dissipated by the flow is inferred using the energy approach (Marot et al., 2012a). This relation involves both the fluid flow rate and the pressure variation in each identified layer in order to estimate the hydraulic loading. This method which combines construction control data and a statistical approach to infer the spatial variation of both the erosion resistance index and of the power dissipated by the flow is an efficient tool to characterize global dam heterogeneities permitting the localization of zones of relatively larger suffusion potential. The detected zones endowed with a lower erosion resistance index and a larger power than their average values, respectively, have a greater suffusion potential (both in amount and in kinetic).

In conclusion for this particular dam, based on the homogeneity of the hydraulic conductivities and on the erosion resistance index values (all  $I_{\alpha} > 5$ ), the overall suffusion potential of this dam appears to be fairly low. Within this positive context, eight zones have been identified with a greater suffusion potential.

#### Acknowledgements

The authors thank the Region Pays de la Loire for providing financial support for this work through the RI-Adaptclim project.

#### References

- Bendahmane, F., Marot, D., & Alexis, A. (2008). Experimental parametric study of suffusion and backward erosion. *Journal of Geotechnical and Geoenvironmental Engineering*, 134(1), 57–67.
- Chang, D. S., & Zhang, L. M. (2012). Critical hydraulic gradients of internal erosion under complex stress states. *Journal of Geotechnical and Geoenvironmental Engineering*, 139(9), 1454–1467.
- Chang, D. S., & Zhang, L. M. (2013). Extended internal stability criteria for soils under seepage. *Soils and Foundations*, 53(4), 569–583.
- Chapuis, R. P. (2004). Predicting the saturated hydraulic conductivity of sand and gravel using effective diameter and void ratio. *Canadian Geotechnical Journal*, 41(5), 787–795.
- Foster, M. (2007). Application of no, excessive and continuing erosion criteria to existing dams. *Internal Erosion of Dams and their Foundations*, Taylor & Francis 1995–2012 LAVOISIER S.A.S., 103–114.
- Foster, M., Fell, R., & Spannagle, M. (2000). The statistics of embankment dam failures and accidents. *Canadian Geotechnical Journal*, 37(5), 1000–1024.
- Fry, J.-J. (2012). Introduction to the process of internal erosion in hydraulic structures: embankment dams and dikes. *Erosion of Geomaterials*, ISTE Ltd and John Wiley & Sons, Inc., 1–37.
- Garner, S., & Fannin, R. (2010). Understanding internal erosion: a decade of research following a sinkhole event. *The International Journal on Hydropower & Dams*, 17(3), 93–98.

- Haghighi, I. (2012). Caractérisation des phénomènes d'érosion et de dispersion: développement d'essais et applications pratiques. Ph.D. Thesis. Université Paris-Est
- ICOLD (2013). Internal erosion of existing dams, levees and dykes, and their foundations. Bulletin 164, Volume 1: Internal Erosion Processes and Engineering Assessment.
- Ke, L., & Takahashi, A. (2014). Experimental investigations on suffusion characteristics and its mechanical consequences on saturated cohesionless soil. *Soils and Foundations*, 54(4), 713-730.
- Ke, L., & Takahashi, A. (2014). Triaxial erosion test for evaluation of mechanical consequences of internal erosion. *Geotechnical Testing Journal*, 37(2), 20130049.
- Kenney, T. & Lau, D. (1985). Internal stability of granular filters. *Canadian Geotechnical Journal*, 22(2), 215–225.
- Kovacs, G. (1981). Seepage hydraulic, Elsevier Scientific Publishing Co, Amsterdam.
- Le, V. T. (2017). Development of a new device and statistical analysis for characterizing soil sensibility face suffusion process. PhD thesis, Université de Nantes, France.
- Le, V. T., Marot, D., Rochim, A., Bendahmane, F., & Nguyen, H. H. (2016). Suffusion susceptibility characterization by triaxial erodimeter and statistical analysis. In 8<sup>th</sup> International Conference on Scour and Erosion (ISCE-8). 12-15 September 2016, Oxford, UK., 453–460.
- Le, V. T., Marot, D., Rochim, A., Bendahmane, F., and Nguyen, H. H. (2017). Suffusion susceptibility investigation by energy-based method and statistical analysis. *Canadian Geotechnical Journal*, (999):1–12.
- Leroueil, S., Le Bihan, J.-P., Sebaihi, S., & Alicescu, V. (2002). Hydraulic conductivity of compacted tills from northern quebec. *Canadian Geotechnical Journal*, 39(5), 1039–1049.
- Li, M. (2008). Seepage induced instability in widely graded soils. PhD thesis, University of British Columbia.
- Li, M., & Fannin, J. (2008). Comparison of two criteria for internal stability of granular soil. *Canadian Geotechnical Journal*, 45, 1303–1309
- Malenfant-Corriveau, M. (2016). Propriétés hydrauliques d'un till compacté possédant un faible pourcentage de particules argileuses. Master's thesis, Université Laval.
- Marot, D. & Benamar, A. (2012). Suffusion, transport and filtration of fine particles in granular soil. *Erosion of geomaterials*, ISTE Ltd and John Wiley & Sons, Inc., 39–79.

- Marot, D., Le, V. D., Garnier, J., Thorel, L., & Audrain, P. (2012a). Study of scale effect in an internal erosion mechanism: centrifuge model and energy analysis. *European Journal of Environmental and Civil Engineering*, 16(1), 1–19.
- Marot, D., Bendahmane, F., & Nguyen, H. H. (2012b). Influence of angularity of coarse fraction grains on internal process. *La Houille Blanche, International Water Journal*, 6(2012), 47–53.
- Marot, D., Regazzoni, P.-L., & Wahl, T. (2011). Energy-based method for providing soil surface erodibility rankings. *Journal of Geotechnical and Geoenvironmental Engineering*, 137(12), 1290–1293.
- Marot, D., Rochim, A., Nguyen, H.-H., Bendahmane, F., & Sibille, L. (2016). Assessing the susceptibility of gap-graded soils to internal erosion: proposition of a new experimental methodology. *Natural Hazards*, 83(1), 365–388.
- Moffat, R., & Fannin, J. (2006). A large permeameter for study of internal stability in cohesionless soils. *Geotechnical Testing Journal*, 29(4): 273-279.
- Perzmaier, S., Muckenthaler, P., & Koelewijn, A. (2007). Hydraulic criteria for internal erosion in cohesionless soil. Assessment of risk of internal erosion of water retaining structures: dams, dykes and levees. Intermediate Report of the European Working Group of ICOLD. Technical University of Munich, Munich, Germany, 30–44.
- Phoon, K.-K., & Kulhawy, F. H. (1999). Evaluation of geotechnical property variability. *Canadian Geotechnical Journal*, 36(4), 625–639.
- Reddi, L.N., Lee, I., & Bonala, M.V.S. (2000). Comparison of internal and surface erosion using flow pump test on a sand-kaolinite mixture. *Geotechnical Testing Journal*, 23, 116–122.
- Regazzoni, P.-L., & Marot, D. (2011). Investigation of interface erosion rate by jet erosion test and statistical analysis. *European Journal of Environmental and Civil Engineering*, 15(8), 1167–1185.
- Rochim, A., Marot, D., Sibille, L., & Thao Le, V. (2017). Effects of hydraulic loading history on suffusion susceptibility of cohesionless soils. *Journal of Geotechnical and Geoenvironmental Engineering*, DOI: 10.1061/(ASCE)GT.1943-5606.0001673.
- Rönnqvist, H., Fannin, J. and Viklander, P. (2014). On the use of empirical methods for assessment of filters in embankment dams. *Géotechnique Letters*, 4, 272–282.

- Sherard, J. L., & Dunnigan, L. P. (1989). Critical filters for impervious soils. *Journal of Geotechnical Engineering*, 115(7), 927–947.
- Skempton, A., & Brogan, J. (1994). Experiments on piping in sandy gravels. *Géotechnique*, 44(3), 449–460.
- Smith, M. (2000). Analyse thermique et géostatistique d'un noyau de barrage en remblai. Master's thesis, Université Laval.
- Smith, M., & Konrad, J.-M. (2011). Assessing hydraulic conductivities of a compacted dam core using geostatistical analysis of construction control data. *Canadian Geotechnical Journal*, 48(9), 1314–1327.
- Tomlinson, S. S., & Vaid, Y. P. (2000). Seepage forces and confining pressure effects on piping erosion. *Canadian Geotechnical Journal*, 37(1), 1-13.
- U.S. Army Corps of Engineers (1953). Filter experiments and design criteria. Technical Memorandum, 3-360, Waterways Experiment Station, Vicksburg.
- Wan, C.F. & Fell, R. (2008). Assessing the potential of internal instability and suffusion in embankment dams and their foundations. *Journal of Geotechnical and Geoenvironmental Engineering*, 134(3): 401-407.
- Watabe, Y., Leroueil, S., & Le Bihan, J.-P. (2000). Influence of compaction conditions on pore-size distribution and saturated hydraulic conductivity of a glacial till. *Canadian Geotechnical Journal*, 37(6), 1184–1194.
- Zhong, C. H., Le, V. T., Bendahmane, F., Marot, D., & Yin, Z. Y. (2017). Investigation of spatial scale effects on suffusion susceptibility. (under review).